

## Supercontinuum Generation in Gases

P. B. Corkum and Claude Rolland

*Division of Physics, National Research Council of Canada, Ottawa, Ontario K1A0R6, Canada*

and

T. Srinivasan-Rao

*Brookhaven National Laboratory, Upton, New York 11973*

(Received 11 June 1986)

Supercontinua extending from the ultraviolet to the infrared are observed from high-pressure (1–40 atm) Ar, Kr, Xe, H<sub>2</sub>, N<sub>2</sub>, or CO<sub>2</sub> illuminated with 2-psec or 70-fsec, 0.6- $\mu$ m pulses with an energy  $\lesssim 500$   $\mu$ J. The blue spectral component is shown to display a nearly universal behavior for all gases and pulse durations. Although the maximum intensity of the focused, femtosecond pulse in an evacuated cell was  $\sim 10^{13}$  W/cm<sup>2</sup>, continuum generation was only observed with the femtosecond pulse when the threshold for self-focusing was exceeded.

PACS numbers: 42.65.Jx, 32.80.-t

Discovered<sup>1</sup> in 1970, supercontinuum generation has now been demonstrated in a wide variety of solids and liquids. Self-phase modulation, four-wave mixing, and plasma production (for the blue spectral component) are the processes most commonly invoked to explain continuum generation.<sup>2</sup> Recent plane-wave theoretical models based on cubic nonlinearities<sup>2,3</sup> describe continuum generation in terms of a parameter  $Q = \eta_2 E^2 z / c \tau$ , where  $\eta_2$  is the nonlinear refractive index,  $E$  is the incident laser field amplitude,  $z$  is the interaction length,  $\tau$  is the pulse duration, and  $c$  is the speed of light. For small  $Q$ , the continuum bandwidth is given by  $\Delta\omega \sim Q\omega$ . A value of  $Q \gtrsim 1$  is required for the generation of a broad ( $\delta\nu \sim \nu$ ) supercontinuum.<sup>2,3</sup>

Experimentally, self-focusing (the spatial analog of self-phase modulation) is difficult to avoid. Self-focusing limits the validity of current  $\eta_2$  continuum theories to

$$Q < (4/\tau)(\eta_2 P / c^3 \epsilon_0 \pi)^{1/2}, \quad (1)$$

where  $P$  is the laser power. Equation (1) is obtained by the requirement that the interaction length be less than the self-focusing length for a Gaussian beam and by the assumption of only full-beam self-focusing. Microfilamentation lowers  $Q$  even further.<sup>4</sup> Although no continuum-generation experiments have clearly satisfied the inequality in Eq. (1), the parameter  $Q$  is used as a guide to estimate the expected spectral broadening. Based on this parameter, gases are not likely to be sources of supercontinua. For example, xenon, a highly nonlinear gas, has a nonresonant  $\eta_2 = 4 \times 10^{-26}$  m<sup>2</sup>/V<sup>2</sup> at atmospheric pressure<sup>5</sup> ( $\eta_2$  of water is  $1.5 \times 10^{-22}$  m<sup>2</sup>/V<sup>2</sup>). If we consider the maximum field that can be applied to Xe in the absence of breakdown<sup>6</sup> ( $I \sim 10^{13}$  W/cm<sup>2</sup>) then, even with a 100-fsec (2 psec) pulse, an interaction length of  $z = 6 \times 10^3$  cm ( $1.2 \times 10^5$  cm) is required for  $Q \approx 1$  in 1-atm xenon. It is not surprising that supercontinuum generation has not been predicted for gaseous media.

This Letter is the first report of supercontinua from gases. Significant spectral broadening has been previously observed by use of 350-fs, 308-nm pulses, and, in in-

dependent work, supercontinua have recently been produced in high-pressure gases by this group as well.<sup>7</sup> We observe continua extending from the ultraviolet to the infrared when picosecond or femtosecond 0.6- $\mu$ m pulses are focused into high-pressure gases. Continua are produced in the rare gases Ar, Kr, and Xe and the molecular gases H<sub>2</sub>, N<sub>2</sub>, and CO<sub>2</sub>. Supercontinua are seen with input powers as low as  $6 \times 10^7$  W in 40-atm Xe and at pressures as low as 1-atm Xe with an input power of  $3 \times 10^9$  W. Within the parameter range of our experiment, we see no continuum from neon. Neon is the only gas that we have investigated in which continuum generation was absent.

The ultrashort 2-psec or 70-fsec pulses used in this experiment are described elsewhere.<sup>8</sup> The pulses were focused into a 90-cm-long high-pressure cell with an  $f/170$  lens to an estimated focal-spot diameter of 100  $\mu$ m. Allowing for optics losses, the incident 70-fsec (2 psec) pulse had a maximum energy of 350  $\mu$ J (500  $\mu$ J), with 70% of this energy in the Airy disk. The transmitted beam was recollimated and dispersed with either (i) a 1-nm/mm spectrograph and recorded on Polaroid film, or (ii) a 10-nm/mm spectrograph and displayed on an optical multichannel analyzer (OMA). Figure 1 shows typical continuum spectra obtained by use of the 70-fsec pulse with a cell pressure of 30-atm xenon (crosses) and using the 2-psec pulse with a cell pressure of 15-atm xenon (circles) or 40 atm of N<sub>2</sub> (squares). The curves represent the average of 25 shots. Corrections have been made for the spectral characteristics of all components.

The similarity of the blue spectral component under these widely different conditions is striking. In fact, the blue spectral component is nearly universal for all gases which produce continua and for all (above-threshold) pressures and intensities.

Because of the limited range of our photocathode the uv component of the continuum was investigated on film. Again there is remarkable uniformity, with the minimum resolvable wavelength varying from 330 nm in CO<sub>2</sub> to 290 nm in Xe. In all gases this "cutoff" wavelength was independent of the intensity. Only for Xe did we see a

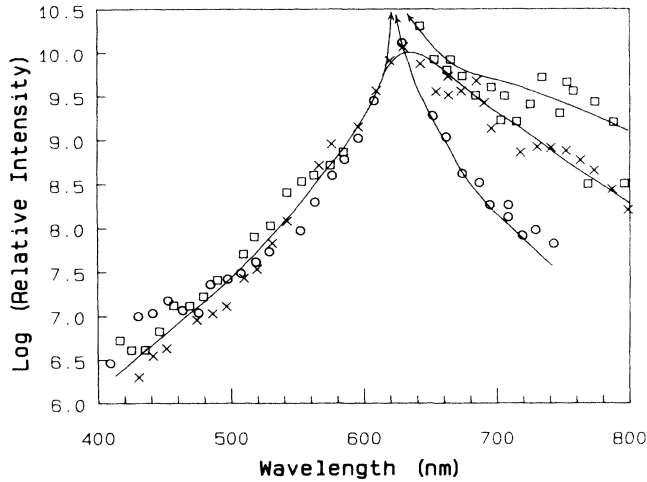


FIG. 1. Continuum spectra. Xenon:  $P=30$  atm,  $P=70$  fsec (crosses);  $P=15$  atm,  $P=2$  psec (circles).  $N_2$ :  $P=40$  atm,  $\tau=2$  psec (squares).

weak density dependence, varying from 290 nm at 1 atm to 330 nm at 35 atm.

As can be seen from Fig. 1, the red spectral component varies from gas to gas and for different intensities and pressures. The maximum wavelength obtained using 30-atm  $CO_2$  illuminated with the 70-fsec pulse, exceeded the limit of an S1 photocathode ( $1.3 \mu m$ ). We did not investigate the maximum wavelength of the other gases.

In all cases, supercontinuum generation showed a sharp threshold, below which only modest broadening occurred and above which full spectra were produced. Figure 2 is a plot of the threshold  $(pP)_{Th}$  as a function of the laser power ( $P$ ) for different gases under femtosecond illumination, where  $p$  is the gas pressure. The product  $(pP)_{Th}$  remains constant as the laser power is changed by a factor of as much as 30 and is proportional to the

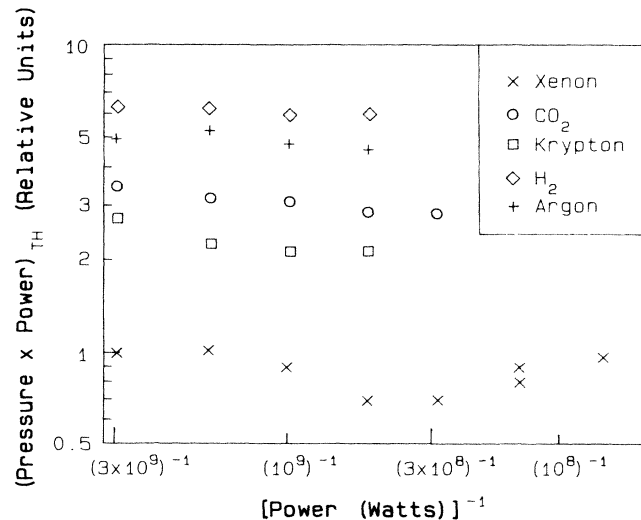


FIG. 2. Pressure times power at threshold, plotted as a function of the inverse of the laser power for different gases.

third-order hyperpolarizability  $\gamma^{(3)}$  of the different gases.<sup>5</sup>  $\gamma^{(3)}$  determines the threshold for continuum generation in all gases except for  $CO_2$  and  $N_2$  with the picosecond pulse. (For  $CO_2$  there is some evidence of the importance of the Raman active mode.)

We account for the sharp threshold by the assumption that self-focusing is essential for continuum generation [see Eq. (1)]. Then the self-focusing threshold, occurring at a power  $P_c = \pi \epsilon_0 c^3 / \eta_2 \omega^2$  for a diffraction-limited Gaussian beam, would equal the threshold power for continuum generation at a given pressure. Experimentally, the two thresholds agree within 20%. The absence of self-focusing in low  $\gamma^{(3)}$  gases accounts for the lack of continuum generation in neon.

Although self-focusing correlates with continuum generation, the beam divergence of the continuum does not increase very much from the beam divergence of the input beam. Figure 3 shows the increase in the beam

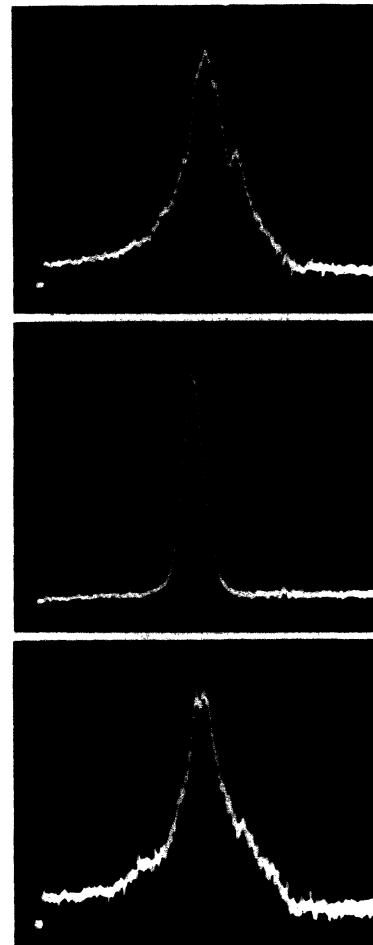


FIG. 3. Spatial distribution of the blue spectral component  $500 \text{ nm} < \lambda < 300 \text{ nm}$  (lower trace), the transmitted beam with the gas cell evacuated (middle trace), and the red spectral component  $1.1 \mu m > \lambda > 0.65 \mu m$  (upper trace). Both the upper and lower traces were taken with 15-atm xenon and a 2-psec input pulse with a power of  $350 \times 10^6 \text{ W}$ . The width is proportional to the beam divergence.

divergence for the 2-psec pulse in xenon. The measurements were made by placing the OMA at the output of the high-pressure cell in place of the recollimating lens (approximately 75 cm from the beam waist). The beam cross section was sampled with use of a 250- $\mu\text{m}$ -wide slit in front of the OMA. Figure 3 (middle trace) shows the incident beam diameter measured at the output of the cell. Figure 3 also shows the diameter of the red (upper trace) and blue (lower trace) components with a Xe pressure of 17 atm. Both traces were obtained with use of appropriate cutoff filters and represent the average of about 50 shots. The operating pressure was approximately four times the threshold pressure. From Fig. 3 we see that the beam diameter (and consequently the beam divergence) of the red or blue components is approximately twice that of the incident beam. (On a single shot the beam divergence can be as low as the incident beam divergence.)

In addition to the above results, any theory of continuum generation in gases must be consistent with the nearly full transmission of the energy through the cell (transmission  $>90\%$ ).

If we postulate that the same mechanism(s) is responsible for the low- and high-pressure results and for the long- and short-pulse results, then we can judge possible explanation(s) against the experimental extremes. We have already discussed continuum generation due to plane-wave  $\eta_2$  processes and noted that even at the accepted breakdown intensity in Xe they were far short of accounting for the continuum bandwidth. In addition, our experimental data do not show the expected dependence of the continuum bandwidth on  $\eta_2$  and  $\tau^{-1}$ . This relationship is fundamental to the theory.

The second mechanism usually suggested as contributing to the formation of the continuum is plasma generation. In condensed media plasma formation is thought to play two roles: First, it limits the size of self-focusing filaments or foci and second, it is an important source of the blue component of the continuum.<sup>9</sup> We demonstrate that the maximum intensity of our 70-fsec pulse cannot be limited at  $10^{13}$  W/cm<sup>2</sup> by plasma formation and that plasma production cannot directly account for significant spectral broadening for any pulse duration until an intensity in excess of  $I \sim 10^{15}$  W/cm<sup>2</sup> is reached.

As in Ref. 9, we assume that stabilization occurs when  $\eta_2 E^2$  equals the plasma nonlinearity<sup>10</sup>  $\frac{1}{2}(N_e/N_c)$ , where  $N_e$  is the electron density and  $N_c$  is the critical electron density.<sup>11</sup> It is possible to express  $N_e$  and  $E^2$  in terms of measurable quantities. Under the assumption of Gaussian optics, the beam waist  $\omega_0$  is related to the confocal parameter  $z_0$  by  $z_0 = \pi\omega_0^2\lambda^{-1}$ , where  $\lambda$  is the laser wavelength. The experimental parameters place an upper bound of  $\omega_0 < (\beta c \epsilon_0 \lambda \tau / 8\pi \eta_2 N_c \alpha E_0)^{1/2}$  on the waist of a Gaussian beam stabilized over  $2z_0$ .  $\beta$  is the fraction of energy extracted from the incident beam,  $E_0$  is the ionization energy, and  $\alpha$  is a fraction, greater than 1, which allows for hot-electron production.<sup>12</sup> Using  $\beta = 0.1$  and

$\alpha E_0 = 15$  eV, we calculate  $\omega_0 < 40$   $\mu\text{m}$  for 1-atm Xe. For an input power of  $2 \times 10^9$  W, plasma stabilization is only consistent with experimental parameters for a breakdown threshold at  $I > 10^{14}$  W/cm<sup>2</sup>. If the same calculation is made for high-pressure Xe (gases) or for H<sub>2</sub>O (condensed media) the stabilization diameter would be much smaller and the breakdown threshold much higher.

The assumption that the beam remains stabilized over a  $2z_0$  may seem restrictive since plasma production could defocus the beam. However, for plasma to modify the beam divergence of a 0.6- $\mu\text{m}$  pulse by only one diffraction-limited beam divergence (equivalent to a  $\pi$  phase change) an integrated plasma density of  $\int N_e dl = 1.8 \times 10^{17}$  cm<sup>-2</sup> is required. By use of  $\beta = 0.1$ ,  $\alpha E_0 = 15$  eV, and  $\tau = 70$  fsec, the beam intensity for measurable defocusing must be  $I = 6 \times 10^{13}$  W/cm<sup>2</sup>. Thus, plasma stabilization (or defocusing) is incompatible with the Xe multiphoton ionization threshold of  $\sim 10^{13}$  W/cm<sup>2</sup>. We will now show that the high plasma-production rate required for significant frequency shifting is also incompatible with the experimental observations.

The frequency shift due to plasma production<sup>13</sup> is given by

$$\Delta\omega = \frac{\pi}{\lambda} \frac{\eta_0}{N_c} \frac{d}{dt} \int N_e(t) dl, \quad (2)$$

where  $\eta_0$  is the linear refractive index ( $\eta_0 \sim 1$  for gases). We can express  $d/dt \int N_e(t) dl$ , which we do not measure, in terms of the beam intensity  $I(t)$ . Then Eq. (2) can be rewritten as

$$\Delta\omega = \frac{\pi}{\lambda} \frac{\eta_0}{N_c} \frac{\beta I(t)}{\alpha E_0}, \quad (3)$$

and is valid for any medium and any pulse duration. Substituting  $\Delta\omega = \omega$ ,  $\alpha E_0 = 15$  eV, and  $\beta = 0.1$ , we obtain  $I(t) = 6 \times 10^{15}$  W/cm<sup>2</sup>, much larger than the multiphoton ionization threshold intensity of  $I = 10^{13}$  W/cm<sup>2</sup>, and defocusing intensity of  $I \sim 10^{14}$  W/cm<sup>2</sup>. Aside from the above reasons, we can eliminate plasma production as the direct cause of the blue spectral component because plasma production, even combined with four-wave mixing, cannot account for a spectrum predominantly shifted to the red.

Our introductory analysis was based on the expected breakdown threshold in Xe, a number that has not been confirmed experimentally for such a short pulse. The measurements reported here imply that the threshold is either much larger than  $10^{13}$  W/cm<sup>2</sup> or that other nonlinear processes become important at intensities lower than the ionization threshold. However, an ionization threshold of even  $10^{14}$  W/cm<sup>2</sup> would not alter the basic conclusion that current plasma or  $\eta_2$  theories cannot account for continuum generation in gases.

Well-controlled experiments are required to determine ionization rates with femtosecond pulses<sup>14</sup> in both low- and high-pressure gases. Aside from their intrinsic interest, these are important because continuum generation

may well result from very high-order nonlinear processes similar to those that manifest themselves in multiphonon ionization. Many experiments<sup>15</sup> indicate that at  $I \gtrsim 10^{13}$  W/cm<sup>2</sup>, the perturbation expansion of multiphoton ionization converges only weakly, if at all. Since the theory of nonlinear optics is similar to that of multiphoton transitions (ionization), we must also expect the traditional perturbation expansion of nonlinear optics to converge weakly, if at all. Qualitatively, multiwave mixing is as likely, or more likely, than four-wave mixing. Thus high-order effects should dominate spectral broadening at very high intensities. Inhibited ionization<sup>16</sup> would only accentuate this process.

In conclusion, continuum generation is a ubiquitous response of most and probably all materials to very high-power short pulses. Whatever theory is eventually developed, it will not depend upon the detail spectroscopy of the medium, but will have a very general form.

We acknowledge the expert assistance of D. Joines and G. Berry throughout this experiment.

---

<sup>1</sup>R. R. Alfano and S. L. Shapiro, Phys. Rev. Lett. **24**, 592 (1970).

<sup>2</sup>G. Yang and Y. R. Shen, Opt. Lett. **9**, 510 (1984).

<sup>3</sup>J. T. Manassah, M. A. Mustafa, R. R. Alfano, and P. P. Ho, IEEE J. Quantum Electron. **22**, 197 (1986).

<sup>4</sup>In water the critical power is  $P \sim 10^6$  W. Many continuum

experiments exceed this threshold by more than  $10^3$  and are, therefore, highly susceptible to microfilamentation.

<sup>5</sup>H. J. Lehmeyer, W. Leupacher, and A. Penzkofer, Opt. Commun. **56**, 67 (1985).

<sup>6</sup>P. Lambropoulos, Phys. Rev. Lett. **55**, 2141 (1985).

<sup>7</sup>J. H. Glowina, G. Arjavalingam, P. P. Sorokin, and J. E. Rothenberg, Opt. Lett. **11**, 79 (1986); P. P. Sorokin, private communication.

<sup>8</sup>C. Rolland and P. B. Corkum, Opt. Commun. **59**, 64 (1986).

<sup>9</sup>N. Bloembergen, Opt. Commun. **8**, 285 (1973).

<sup>10</sup>P. B. Corkum and D. Keith, J. Opt. Soc. Am. B **2**, 1873 (1985).

<sup>11</sup>The change in the refractive index due to ion generation has not been considered. However, in large-atomic-number systems such as Xe, the refractive index of ions and neutral atoms is not expected to differ significantly. Hence, in view of the low plasma density, ion production should not contribute much to continuum generation.

<sup>12</sup>L. A. Lompré, A. L'Huillier, G. Mainfray, and C. Manus, J. Opt. Soc. Am. B **2**, 1906 (1985).

<sup>13</sup>P. B. Corkum, IEEE J. Quantum Electron. **21**, 216 (1985).

<sup>14</sup>Above the self-focusing threshold, the moving focus produces a shorter, effective pulse duration as viewed by an on-axis molecule in the focal region.

<sup>15</sup>See, for example, *Multiphoton Ionization of Atoms*, edited by S. L. Chin and P. Lambropoulos (Academic, New York, 1984).

<sup>16</sup>D. J. Jackson and J. J. Wynne, Phys. Rev. Lett. **49**, 543 (1982).

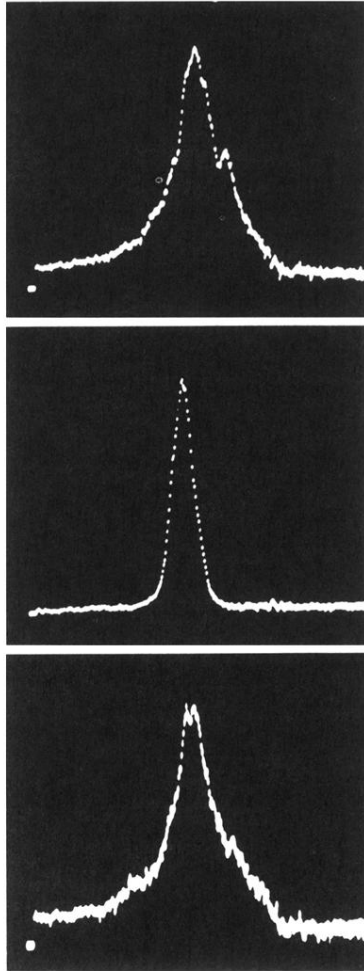


FIG. 3. Spatial distribution of the blue spectral component  $500 \text{ nm} < \lambda < 300 \text{ nm}$  (lower trace), the transmitted beam with the gas cell evacuated (middle trace), and the red spectral component  $1.1 \mu\text{m} > \lambda > 0.65 \mu\text{m}$  (upper trace). Both the upper and lower traces were taken with 15-atm xenon and a 2-psec input pulse with a power of  $350 \times 10^6 \text{ W}$ . The width is proportional to the beam divergence.